

## Supporting Information

# **Enhancing the Performance of Organic Solar Cells and Polymer Light Emitting Diodes via a Novel Giant Polyoxomolybdate Bifunctional Interlayer Material**

Jing Qiu<sup>a</sup>, Yan Wang<sup>a</sup>, Guofeng Wan<sup>a</sup>, Zilong Bing<sup>a</sup>, Huiru Liu<sup>a</sup>, Bing Li<sup>a</sup>, Chengzhuo Yu<sup>a</sup>, Jinyu Zhu<sup>a</sup>, Donal D.C. Bradley<sup>b,c</sup>, Jingsong Huang<sup>b\*</sup>, Lixin Wu<sup>a\*</sup> and Fenghong Li<sup>a\*</sup>

<sup>a</sup> *State Key Laboratory of Supramolecular Structure and Materials, College of Chemistry, Jilin University, Changchun 130012, China*

<sup>b</sup> *Oxford Suzhou Centre for Advanced Research, University of Oxford, Suzhou 215123, China*

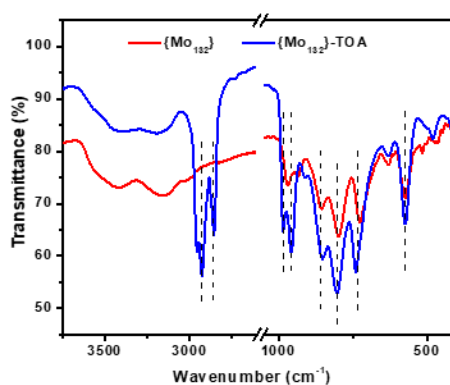
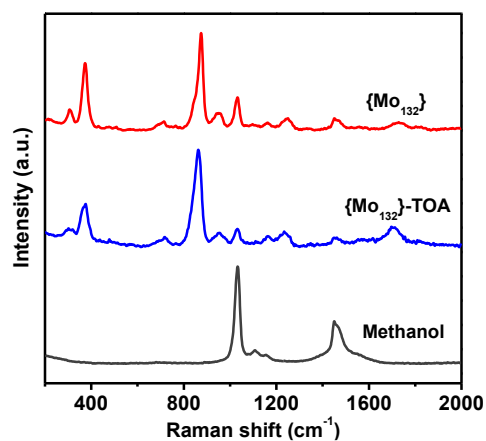
<sup>c</sup> *NEOM Education, Research, and Innovation Foundation, Neom Community 1, Building 4758, Al Khuraybah, Tabuk Province, KSA 49643*

\*Corresponding author.

*E-mail address:* jingsong.huang@oxford-oscar.cn (J. S. Huang); wulx@jlu.edu.cn (W. L. Wu); fhli@jlu.edu.cn (F. H. Li).

**Table S1** Elemental analysis calculated for {Mo<sub>132</sub>}-TOA

Element	C (%)	H (%)	N (%)
Found	33.53	6.47	1.32
Calculated	33.81	6.62	1.58
Error	-0.28	-0.15	-0.26
Fitting Structure	$((C_8H_{17})_4N)_{31}(NH_4)_{11}[Mo_{132}O_{372}(CH_3COO)_{30}(H_2O)_{72}]$		

**Figure S1** Fourier transform infrared spectrum of {Mo<sub>132</sub>} and {Mo<sub>132</sub>}-TOA.**Figure S2** Raman spectrum of {Mo<sub>132</sub>} and {Mo<sub>132</sub>}-TOA. The spectrum for methanol, the solvent used to deposit the films, is also shown.

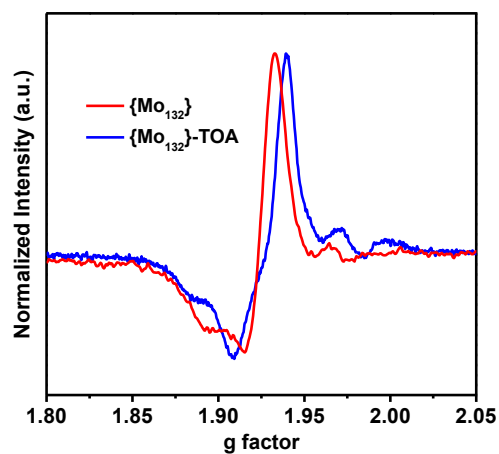


**Figure S3** Electron paramagnetic resonance spectrum of  $\{\text{Mo}_{132}\}$  and  $\{\text{Mo}_{132}\}$ -TOA.

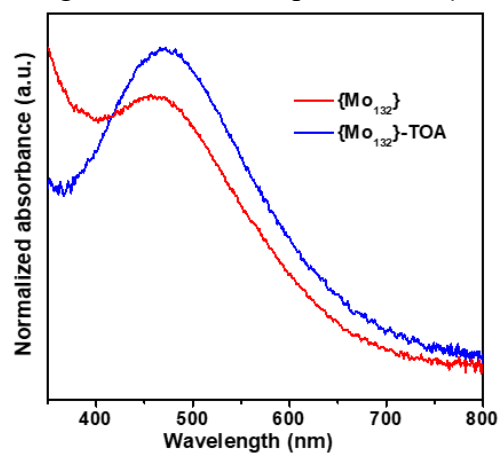


**Figure S4** Ultraviolet-visible absorption spectrum of  $\{\text{Mo}_{132}\}$  and  $\{\text{Mo}_{132}\}$ -TOA on ITO substrate.

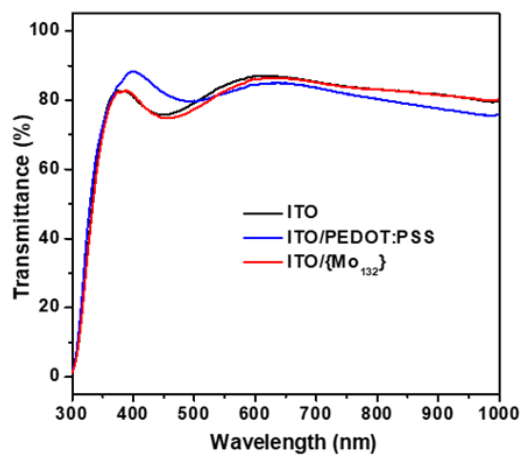


**Figure S5** Transmittance spectrum of ITO, ITO/PEDOT:PSS and ITO/ $\{\text{Mo}_{132}\}$ .

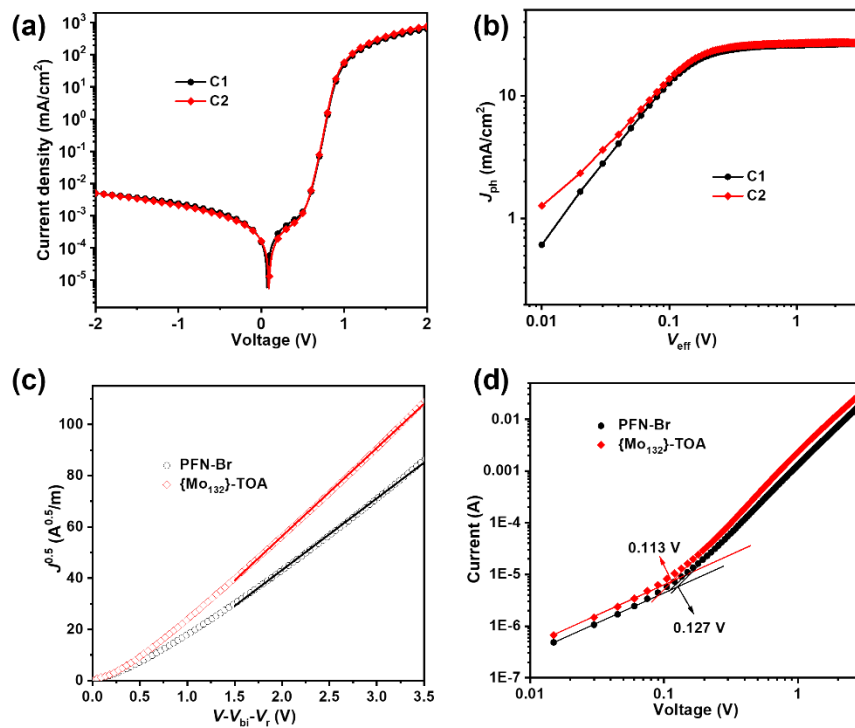


**Figure S6** (a) The dark state  $J$ - $V$  curves and (b)  $J_{ph}$ - $V_{eff}$  curves of devices C1 and C2. The  $J_{0.5}$ - $V$ - $V_{bi}$ - $V_r$  curves and  $I$ - $V$  curves of the ITO/ZnO/PM6:Y6/CIL/Al single electron device.

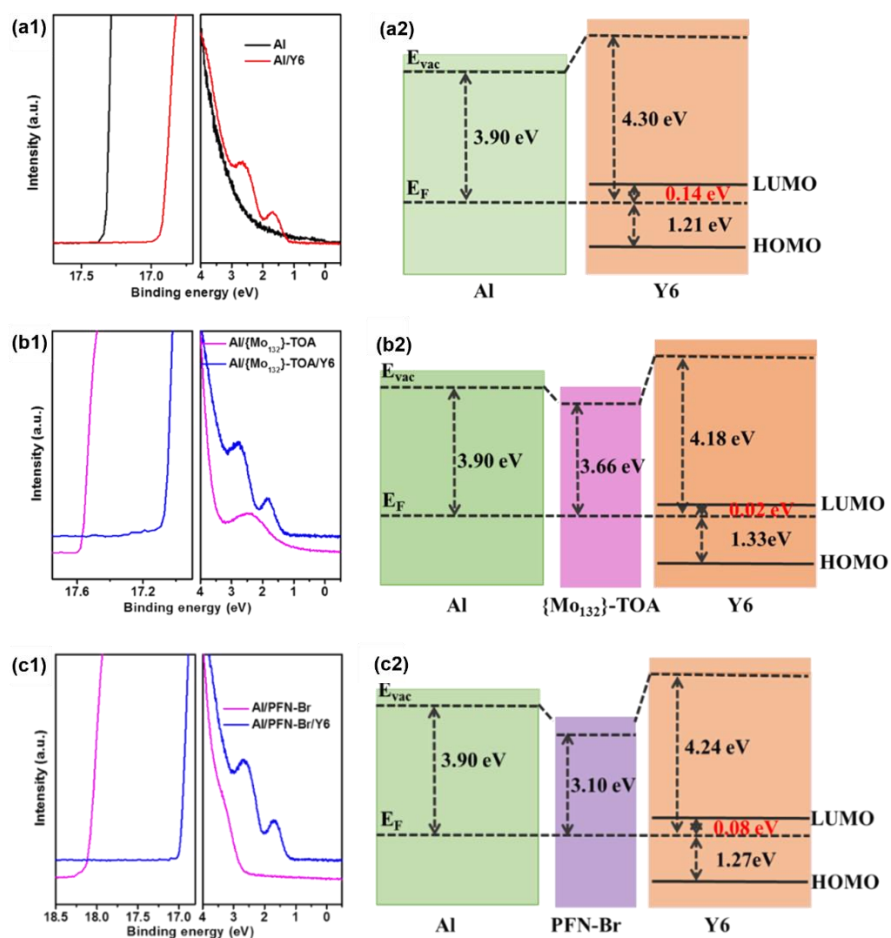


**Figure S7** (a1) UPS spectra and (b1) band bending diagrams of Al/Y6. (b1) UPS spectra and (b2) band bending diagrams of Al/{Mo<sub>132</sub>}-TOA/Y6. (c1) UPS spectra and (c2) band bending diagrams of Al/PFN-Br/Y6.

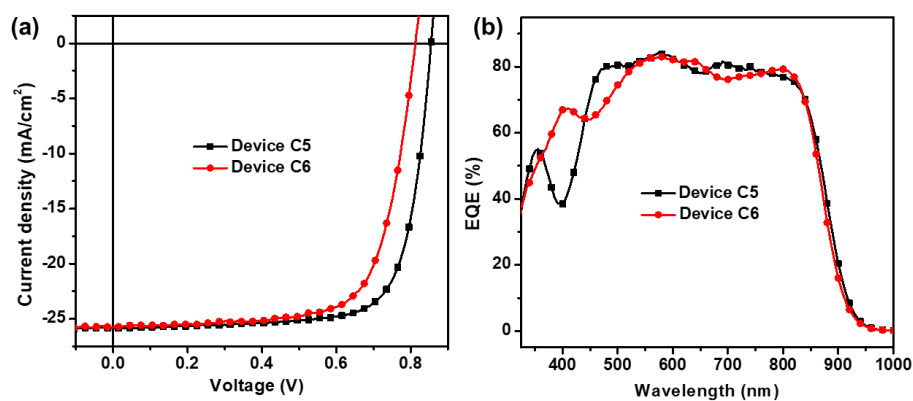


**Figure S8** (a)  $J$ - $V$  curves and (b) EQE spectra of PM6:Y6 based OSCs with Ag.

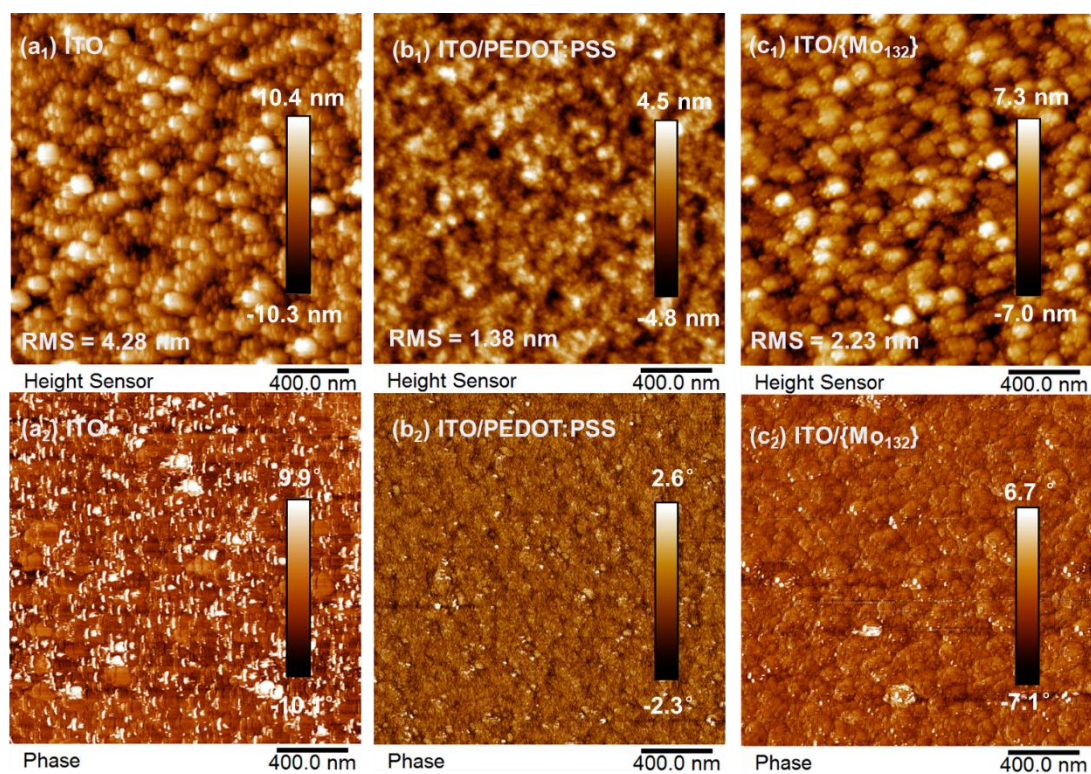


**Figure S9** (a) AFM height images and phase images of ITO (a<sub>1</sub> and a<sub>2</sub>), ITO/PEDOT:PSS film (b<sub>1</sub> and b<sub>2</sub>) and ITO/{Mo<sub>132</sub>} film (c<sub>1</sub> and c<sub>2</sub>).

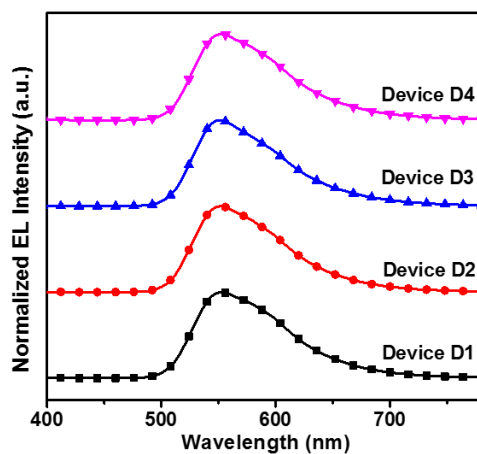


**Figure S10.** The Electroluminescence spectra of PLEDs with different cathode and anode interlayers.

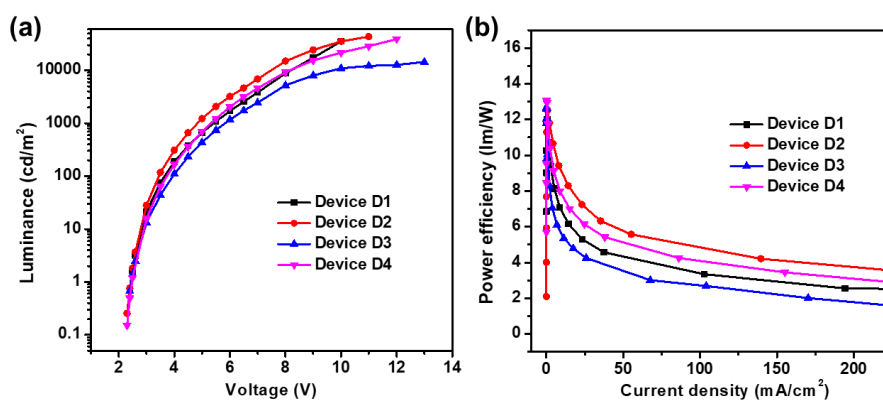


**Figure S11.** (a) luminance-voltage and (b) power efficiency-current density characteristics of Super Yellow based PLEDs with different cathode and anode interlayers.

**Table S2.** Electroluminescence performances of Super Yellow based PLEDs with different cathode and anode interlayers

Device	Turn-on voltage (V)	Max. Luminance (cd/m <sup>2</sup> )	Current efficiency (cd/A)	Power efficiency (lm/W)
D1	2.5	35090	13.67	12.00
D2	2.5	43430	15.24	12.52
D3	2.5	14330	13.41	12.68
D4	2.5	39030	14.95	13.08

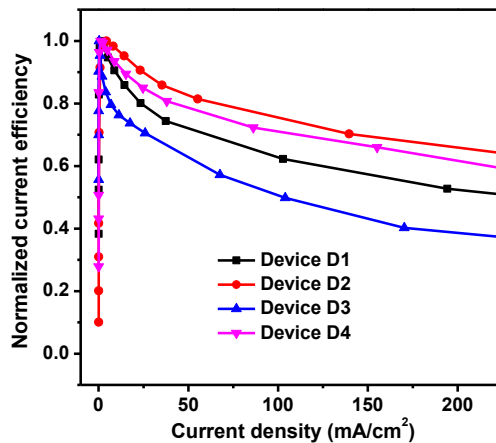


**Figure S12.** Normalized current efficiency-current density characteristics of Super Yellow based PLEDs with different cathode and anode interlayers.